Self-Consistent Field Modeling of Linear Nonionic Micelles

A. B. Jódar-Reyes*,† and F. A. M. Leermakers‡

Departamento de Fısica, Universidad de Extremadura, Facultad de Veterinaria, Avda. de la Universidad s/n, Cáceres, Spain, and Laboratory of Physical Chemistry and Colloid Science, Wageningen University, Dreijenplein 6, 6703 HB Wageningen, The Netherlands

Received: November 21, 2005; In Final Form: January 30, 2006

A self-consistent field theory is used to predict structural, mechanical, and thermodynamical properties of linear micelles of selected nonionic surfactants of the type C_nE_m. Upon increase in surfactant concentration the sudden micelle shape transition from spherical to cylindrical (second critical micelle concentration (cmc)) is analyzed. The cylindrical micelles consist of a body (with radius R_c and length L) and two slightly swollen endcaps. For small L, the shape resembles a dumbbell. With increase in the length of the body, an oscillatory behavior in the grand potential of the micelle is found. The wavelength of the oscillation (λ_d) is proportional to the surfactant tail length n. The amplitude of these oscillations decreases exponentially with a decay length ξ. In the limit of very long micelles, the grand potential converges to the endcap (free) energy E^c. This endcap energy increases approximately quadratic with the tail length and diminishes by increasing the headgroup size m. The micelle size distribution is generated showing non-monotonic features due to the presence of short dumbbells and becomes exponential when $L \gg 8R_c$. It is also shown that the endcap energy can be estimated in first order by the grand potential of the spherical micelle that coexists with infinitely long cylindrical micelles. The persistence length l_p of these linear micelles is evaluated to estimate the relative importance of conformational entropy for these micelles.

Introduction

The focus in this paper is on linear micelles composed of nonionic surfactants in aqueous solution. The issue that we want to address is how the shape of the surfactant micelle changes from spherical to cylindrical by increasing the concentration of surfactants in the system. A molecular-level analysis of this shape transition is presented, and the structural and mechanical properties of the micelles (such as the endcap energy, the persistence length, and the stretching modulus) are analyzed as a function of the surfactant tail length and headgroup size of the alkyl−ethylene oxide C_nE_m family.

On the basis of early static light scattering experiments on ionic surfactants at high salt concentrations,[1] it was concluded that the micelles undergo a transition from spherical to rodlike aggregates upon increase in surfactant concentration above the critical micelle concentration (cmc). This idea has been supported by many experimental works during the past 4 decades, i.e., by using viscosity,[2] turbidity,[3−6] dynamic light scattering.[7−9] pulse gradient spin−echo NMR,[10] and cryo-TEM[10,11] measurements.

Early molecular dynamic (MD) simulation attempts have been made in order to address structural properties of micelles. Despite of the fact that they imposed a given shape of the micelle, the simulations of Haile and O'Connell[12] provided useful information about the segment density distributions and conformational statistics. Other authors[13,14] avoided shape assumptions; however, longer CPU times as well as many more water molecules were required in order to follow spontaneous aggregation in dilute solutions. More recent studies[15,16] improved those simulations. Even though these authors used a coarse grained particle model, many properties of real surfactant solutions were found, including spontaneous micellization in the water phase. From coarse grained MD simulations it is now possible to extract mechanical properties such as the bending modulus (persistence length).[17,18] Detailed MD simulations will not be the endpoint of theoretical investigations. Analytical approaches and partition function methods may provide additional insights in surfactant self-assembly.

Ben-Shaul et al.[19] made a "first order" approach by adopting as a premise the fact that large aggregation numbers are associated with a preference for cylindrical or bilayer packing of amphiphilic molecules. The effect of this premise on the equilibrium size distribution of micellar aggregates and its dependence on the concentration were explored.

There exist statistical-thermodynamic formulations[20−22] of micellar solutions that take into account the role of the solvent, the intra- and intermicelle interactions, or the effects of translational and rotational motions. Hoeve et al.[20] derived possible distributions of micellar sizes with a fairly sharp maximum. They assumed that a spherical shape persisted until the micelle became so large that further growth was impossible without having polar heads in the interior of the micelle. When large micelles were formed, the predicted shape was platelike rather than rodlike. Aranow[21] derived the distribution of clusters at equilibrium in terms of the partition functions for single clusters in the system. Structural properties of the micelles were not included in this theory. Poland et al.[22] discussed the micelle stability in nonionic systems and the variation of the most probable micelle size with the concentration. They assumed that the polar head only served to solubilize the monomers and the micelle in water and did not contribute to the free energy of

* Corresponding author. E-mail address: ajodar@unex.es.
† Universidad de Extremadura.
‡ Wageningen University.

10.1021/jp056737y CCC: $33.50
Published on Web 03/03/2006

the micelle. Unfortunately their method led to formal expressions that only can be solved by using drastic approximations.

An elegant thermodynamic analysis of micellization in nonionic surfactants was developed by Hall et al.[23] as an extension of the small-system thermodynamics of Hill.[24] This treatment, although it was restricted to noninteracting small systems, enabled an evaluation of the partial treatments of the mass-action[25,26] and the phase-separation approaches[27,28] as it embodied aspects of both of them. Other treatments of amphiphilic self-assembly and micellar growth combine basic classical thermodynamics with phenomenological models for the various contributions to amphiphile−amphiphile and amphiphile−water interactions.[29]

The use of computers allows the formulation of a self-consistent field (SCF) theory powerful enough to study self-assembly of surfactants in aqueous solution in a molecularly realistic way. We will apply such an approach called SCF-A,[32] self-consistent-field theory for adsorption and/or association. This statistical approach successfully implements the concepts of the Thermodynamics of Micelle Formation[33] (based on ref 24) to study the association of amphiphilic molecules in solution.[32,34,35] The advantage of applying small-system thermodynamics to micelle formation over alternative approaches is that the actual intrinsic thermodynamic functions of the micelles can be discussed. The aggregation number can be treated as a thermodynamic variable, and the variations in the thermodynamic functions of the micelle formation with, i.e., aggregation number and concentration of micelles, can be analyzed.

Recently, the SCF-A model has been extended to study the shape transition in micellar solutions for nonionic surfactants.[8] These preliminary results support the coexistence of spherical and dumbbell-like micelles, that is, finite size cylindrical micelles with swollen endcaps. This type of structure was proposed by Eriksson[36] on the basis of a detailed analysis of the mechanical equilibrium state of the micelle. It was supported by May et al.[37] They determined the equilibrium shape and energy of the micelle by functional minimization of the total free energy, which is expressed as an integral over local molecular packing free energies in different regions of the micelle. Despite the fact that they consider this theory as a molecular-level one, the local packing free energy per molecule is expressed in terms of macroscopic quantities such as the surface tension or the elastic stretching modulus. Computer simulations have also predicted such a structure.[38] Dumbbell-like micelles have been also seen by transmission electron microscopy at cryogenic temperatures (cryo-TEM) with a dimeric (gemini) surfactant by Bernheim-Groswasser et al.[11] Unlike Eriksson's theory, SCF calculations do not need to specify the position of the headgroups.

An important parameter in linear micelles is the endcap energy E^c, the energy required to create two endcaps from a semi-infinite cylinder. In the case of uncharged micelles, this energy can be also called the scission energy. However, for charged micelles, the energy of scission has an additional term addressing the repulsion of the surface charges.[39] The endcap energy is closely related to the growth of the linear micelles; i.e., when E^c is large, linear micelles become very long, even entangled at relatively low volume fractions of surfactants.[40] Mean fields models[41,42] predict that the number density of elongated micelles of length L is exponential with some mean length. Such a mean length is exponentially dependent on the scission energy. Several works appear in the literature applying this approximation to obtain the scission energy from experiments: for nonionic surfactants (SLS measurements[43]), for ionic surfactants (rheology[44]), for mixtures of ionic surfactants (rheology[45,46]), and for ionic dimeric surfactants (rheology[47]). By using the SCF model, Majhi et al.[8] pointed that the endcap energy could be given (in first approximation) by the grand potential of the spherical micelle coexisting with the rods. They related the existence of forbidden structures with an oscillatory behavior of the grand potential of the micelle upon increase of the micellar aggregation number. This is in disagreement with the general assumption of monotonic growth from spheres to rods with the change of various parameters.[48] However, experimental results using cryo-TEM and pulse gradient spin−echo NMR[10] supported the coexistence of spherical micelles with dimensions independent of concentration and wormlike micelles whose size increased with concentration in dilute solutions of nonionic surfactants. This coexistence has been also seen for a dimeric (gemini) surfactant[11] and by dynamic light scattering with dimethyldodecyldimethylamine oxide at certain pHs and at high ionic strength.[8]

In this paper we extend the work of Majhi et al.[8] and analyze the micellar shape transition in nonionic surfactants by increasing the surfactant concentration and focus on the role of the chain properties in this phenomenon.

Below we will pay detailed attention to the way the cmc is calculated. Two limiting theoretical values are presented by applying two different definitions of the cmc. These two values are expected to bracket the experimental value, where it is understood that in experiments one also expects a cmc region rather than a unique value. The existence of a gap in the size distribution of micelles, between spherical and uniaxial linear micelles, was previously reported by several authors[29,37,49,50] giving rise to the idea of a second cmc. Porte et al. suggested that such a gap was due to the more unfavorable state of the surfactants that are at the junction between the cylindrical body and the endcaps (i.e., at the neck of the micelle). Below we elaborate on this conjecture. They also defined the second cmc as the total surfactant concentration at the transition from short to long linear micelles.[30] Even though our study of these finite size cylindrical micelles was carried out by using the two-gradient (two-dimensional) theory, the possibility of predicting the second cmc by means of the less CPU expensive one-gradient theory is also examined. The influence of the hydrophobic tail and the polar head lengths on the first and second cmc's is analyzed in this article. Regarding the first cmc, we will compare our results with those obtained by Szleifer et al.[31] by using a single-chain mean-field theory in combination with the mass action model.

As the partition function is evaluated accurately in a SCF analysis, we can provide information on the thermodynamics of the dumbbell-like micelles. The damped oscillatory behavior of the grand potential upon increasing the number of surfactants will be examined and related to the characteristics of the surfactant architecture. Two ways to calculate the endcap energy as suggested by ref 8 of linear micelles will be compared systematically. Candau et al.[39] supported that the endcap energy is mainly controlled by the bulkiness of the hydrophobic tails. Others[51] defend that large hydrophobic chains may contribute to high endcap energies. The main role of the hydrophobic tail on the endcap energy will be checked, and the relation between E^c and the tail length n will be established.

Different mechanical properties of the linear micelles are also evaluated (i.e., bending modulus and extendability). The bending modulus is directly related to their persistence length. This value can be used to estimate the conformational entropy of the

wormlike micelles. Although the conformational entropy is typically ignored in the SCF analysis, one can a posteriori test the validity of this assumption.

Finally, to complete the analysis of linear micelles, fluctuations in micelle size are taken into account, and typical examples of the micelle size distribution are generated.

Thermodynamics of Small Systems

A typical micellar solution introduces a macroscopic value for the total surface area between apolar cores and the aqueous solution to a system. In principle classical thermodynamics deals with macroscopic properties of a system. However, unlike the macroscopic interface between an alkane and water phase, the micellar surface is subdivided into many small parts. Therefore it should be considered as an ensemble of small systems. Hill[24] derived the thermodynamic expressions that describe such subsystems at a mesoscopic level. Hall and Pethica[23] successfully applied this theory to the formation of micelles. The one-dimensional SCF-A theory was the first statistical implementation of these ideas for the self-assembly processes.[32] Following the arguments of the Thermodynamics of Small Systems, the macroscopic system, that is, the solution, is divided in $\aleph$ identical, noninteracting small systems. Each small system contains one object (i.e., one micelle). Here the total system is supposed to be monodisperse; however, in the final part of our analysis we will consider the micelle size distribution in detail. The change in the Helmholtz energy of the system containing $\aleph$ small systems is given by

$$\mathrm{d}F = -S\,\mathrm{d}T + V\,\mathrm{d}P + \sum_i \mu_i\,\mathrm{d}n_i + \epsilon\,\mathrm{d}\aleph \qquad (1)$$

where S is the total entropy, V is the total volume, T is the temperature, P is the pressure, μ_i is the chemical potential of component i, n_i is the total number of molecules of i, and $\epsilon\,\mathrm{d}\aleph$ is the subdivision work. The conjugate of the number of small systems is the subdivision potential, ϵ, that represents the energy necessary to divide the system at constant T, P, and number of molecules and is equal to the overall excess free energy of micelle formation. By assuming that the system is incompressible, the following equilibrium condition is found

$$\left(\frac{\partial F}{\partial \aleph}\right)_{P,T,\{ni\}} = \epsilon = 0 \qquad (2)$$

In addition, from the condition of minimum $\partial\epsilon/\partial\aleph > 0$, and as proved,[52] $\partial\epsilon/\partial n^{\mathrm{exc}} < 0$, where n^{exc} is the surfactant aggregation number.

From the definition of the grand potential, $\Delta = \Delta(T,P,\mu_i)$ we have

$$\Delta = \epsilon\aleph \qquad (3)$$

Therefore, ϵ also corresponds to the grand potential per object.

The SCF-A theory is applied to one (average) small system for obtaining this quantity. However, there exists a constraint in the procedure: the micelle has to be fixed in the center of the coordinate system used in the calculations. As a result only the translational restricted subdivision potential can be examined which is denoted by ϵ_{m}. This intrinsic (standard state) grand potential contains detailed information on the self-assembly of surfactants. The direct consequence of having just one micelle in the system is that in the primary SCF analysis the size distribution is not considered. Such analysis is built as an addendum on top of the SCF results.

Again, in SCF calculations one focuses on the most likely micelle. However, it is possible to obtain information on magnitude of the fluctuations in aggregation number. This is easily illustrated. The starting point is to mention that the calculations obey accurately to the Gibbs−Duhem relation

$$\frac{\partial \epsilon_{\mathrm{m}}}{\partial \mu_{\mathrm{surf}}} = -n^{\mathrm{exc}} \qquad (4)$$

where μ_{surf} is the chemical potential of the surfactant. From standard statistical mechanics we know that $kT(\partial\langle n^{\mathrm{exc}}\rangle/\partial\mu_{\mathrm{surf}}) = \langle n^{\mathrm{exc}}\rangle - \langle (n^{\mathrm{exc}})^2\rangle$ where the angular brackets give an ensemble average. Realizing that in eq 4 the aggregation number $n^{\mathrm{exc}} \equiv \langle n^{\mathrm{exc}}\rangle$, we can find

$$\frac{\partial \epsilon_{\mathrm{m}}}{\partial n_{\mathrm{exc}}} = -k_{\mathrm{B}}T\frac{\langle n^{\mathrm{exc}}\rangle}{\langle (n^{\mathrm{exc}})^2\rangle - \langle n^{\mathrm{exc}}\rangle} \qquad (5)$$

Equivalently, $-k_{\mathrm{B}}T\partial n^{\mathrm{exc}}/\partial\epsilon_{\mathrm{m}}$ is related to the relative fluctuations in the micellar aggregation number.

We analyze these fluctuations in micellar size in detail below in our results.

Self-Consistent Field Theory for Self-Assembly. The SCF theory is a statistical thermodynamic treatment that applies a mean-field approximation using a lattice discretization scheme. It was first developed for the adsorption of homopolymers on a solid−liquid interface by Scheutjens and Fleer[53,54] and was subsequently extended to treat copolymers.[32] This theory attempts to describe a three-dimensional (3D) system. By making use of the symmetry in a system, it is possible to implement a mean-field approximation in at least one, but often in two dimensions, leading to a system in which there are two (2D) and often one gradient (1D) in molecular distributions, respectively. The surfactant molecules are represented by a chain of segments with polar or apolar properties. The solvent (water) molecules are much smaller in size and are modeled by a pair of polar segments. A Markov approach is used for generating the conformations of the amphiphilic molecules, which account for segment density gradients in one (1D-SCF approximation[35,53−55]) or two directions (2D-SCF approximation[56−58]).

In the SCF theory, the symmetry of the lattice is preassumed, and as a consequence, the topology of the micelles is to some extend dictated. In this paper we will analyze the thermodynamic and structural properties of micelles with spherical and cylindrical symmetry. Spherical micelles can be studied by using the 1D-SCF theory in spherical geometry (Figure 1b). The primary results are the radial volume fraction profiles denoted by $\varphi(r)$. The center of the lattice corresponds to $r = 0$. Infinitely long cylindrical micelles can be considered by means of the 1D-SCF theory in cylindrical geometry (Figure 1a). Again, the segment density gradients in the radial direction are computed. In this case all the quantities are calculated per unit length of the cylinder. Finite size cylindrical micelles and also the torus-shaped micelle can be generated by using the 2D-SCF theory in cylindrical geometry (Figure 1c). Segment density gradients in the radial direction, r, and in the direction along the axis of the cylinder, z (Figure 1d), are the primary results.

Important quantities are the volume fraction distribution of chain segments, $\varphi(r)$ in 1D and $\varphi(z, r)$ in 2D, and the volume fractions of solvent molecules $\varphi_{\mathrm{W}}(r)$ in 1D and $\varphi_{\mathrm{W}}(z,r)$ in 2D. In the bulk, these values are φ^{b} and $\varphi_{\mathrm{W}}{}^{\mathrm{b}}$. The volume fractions of the surfactant molecules can be split into that corresponding to apolar units $\varphi_{\mathrm{C}}(r)$ or $\varphi_{\mathrm{C}}(z, r)$ and that due to polar units $\varphi_{\mathrm{O}}(r)$ and $\varphi_{\mathrm{O}}(z,r)$. Conjugated to the volume fractions per segment

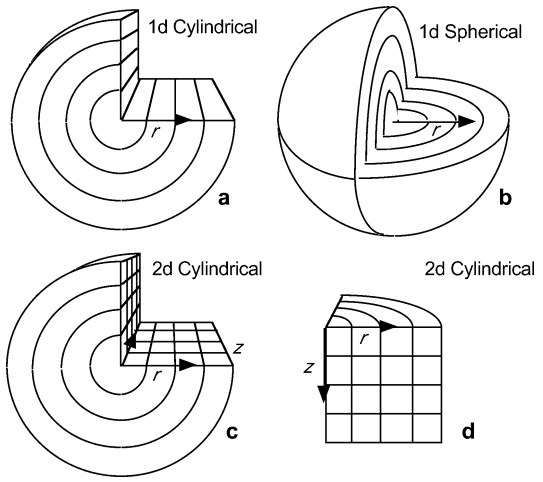

Figure 1. Different lattice geometries in SCF calculations: (a) 1D cylindrical geometry; (b) 1D spherical geometry; (c and d) 2D cylindrical geometry.

type $\varphi_X(z,r)$, there are segment potentials $u_X(z,r)$, where X = C, O, W. These potentials include excluded-volume contributions such as the short-range nearest-neighbor contact energies parametrized by Flory−Huggins interaction parameters. In the present system, interactions between the segments forming the chains as well as solvent−surfactant segment interactions are considered. The SCF formalism gives rules for how to compute the segment volume fractions from the potential on one hand and how to compute the potentials from the segment densities on the other hand. The mutual consistency is generated numerically[32] taking the constraint $\sum_X \varphi_X(z,r) = 1\ \forall z,r$ into account. From the self-consistent solution, the structure of the micelle is obtained and, in addition, it is possible to evaluate the partition function and, from this, all thermodynamic quantities such as the grand potential and the chemical potentials.[55] Typically, the volume fractions are obtained with seven significant numbers and the grand potential has at least five significant numbers. We refer to the literature for further details, i.e., for the 1D-SCF[34] and 2D-SCF[58] approaches.

The Parameters. Any molecular level theory needs a set of parameters. In this case there exist lattice parameters, parameters associated with the structure of the molecules, and quantities that specify the interactions. First, a lattice parameter (λ) is introduced which specifies the mixing of local with nonlocal interactions, i.e., in the contact energy evaluation. In our calculations we used $\lambda = 1/3$, which is optimal to prevent so-called lattice artifacts. Each segment in the surfactant chain is supposed to be of the size of a lattice site *l*. Below, all linear lengths are given in units *l*, and we advise to implement a value of approximately $l \approx 0.2$ nm (corresponding to the size of a united atom CH_2) to convert lattice units to real dimensions.

Our calculations are carried out for several nonionic surfactants with a linear structure, $C_n(OC_2)_mO$, abbreviated as C_nE_m, where C is the apolar unit and O is the polar one. Tail length effects were checked by studying chains with different tail length (n = 12, 14, 16, and 18) and fixed head length (m = 8). Similarly, head size effects were examined with chains of n = 12 and m = 4, 6, and 8. The second component is water, modeled as a dimer (W_2) (water is larger than a C group). Regarding the interaction parameters, the most important one for the self-assembly of surfactants is that for the hydrocarbon−water interaction. The value $\chi_{CW} = 1.5$ is chosen because it reproduces semiquantitatively the experimentally found decrease of the cmc with increasing chain length.[59] The hydrophilicity of the headgroup is ensured by choosing $\chi_{OW} = -0.5$. Finally, the parameter $\chi_{CO} = 2.2$ reflects a repulsive interaction between the hydrophobic tail and the hydrophilic headgroups. This set of parameters resembles the one used in previous studies. We note however that we do not insist on the exact values of these parameters. Instead we focus on trends.

Results and Discussion

1D-SCF Prediction of the First and Second cmc. The definition of the critical micelle concentration (cmc) is quite arbitrary because the first appearance of micelles is not a first-order phase transition. In principle, a practical definition should be simple to handle mathematically and should correspond to a concentration easily identified by experiment. Corrin[60] defined this critical concentration in terms of the reversible aggregation process: "the critical concentration represents the total concentration of long-chain electrolyte at which, for compounds possessing the same polar headgroup, a small and constant number of long-chain ions are in aggregate form". This definition implies that the number of aggregated ions at the critical concentration for a homologous series of paraffin chain salts is thus independent of the hydrocarbon chain length. This is in agreement with the nature of the end-point in the determination of critical concentrations by the dye spectral method. Phillips[61] defined the cmc as the point corresponding to the maximum change in gradient in an ideal colligative property−total surfactant concentration curve. This definition has been adopted by several authors.[25] The phase-separation model establishes the cmc as the saturation concentration of the surfactant monomer in solution with respect to the micellar phase. Discontinuities in physical properties plotted versus concentration should be found at the cmc. However, experiments show that the cmc is not always very sharp. Along lines similar to Phillips', Small System Thermodynamics[23] points out a slight variation in the concentration of monomers with total concentration even when micelles are present. Furthermore, the micellar weight can change with total surfactant concentration.

Very often the pragmatic assumptions are made that the cmc is relatively sharply defined and that above the cmc the monomer concentration is constant. Transport measurements have shown that these two assumptions are really not very good[62] and also the SCF analysis in combination with the analysis of micelles according to the thermodynamics of small systems shows that the cmc cannot uniquely be defined.

In the SCF-A theory, the key thermodynamic quantity is the translational restricted grand potential ϵ_m of the micelle which is a function of its size, that is, the surfactant aggregation number n^{exc}: $\epsilon_m(n^{exc})$. At equilibrium, following eq 2, ϵ_m must be compensated by entropy terms which account for the translational freedom of the center of mass. This leads, for low micelle concentrations (near the cmc), to $\varphi_m = \exp(-\epsilon_m(n_{exc})/k_BT)$ where φ_m is the volume fraction of micelles in the system.[52] Here, we highlight that only most likely micelles are considered in this discussion. Further on in this paper, we will redefine the expression for calculating the volume fraction of micelles in the system by taking into account the fluctuations in micelle size.

At the cmc, the concentration of micelles is minimum. Therefore, ϵ_m must be high and also, $\partial\epsilon_m/\partial n^{exc} < 0$ for having stable equilibrium. Consequently, this point coincides with a maximum of $\epsilon_m(n^{exc})$. The value of φ^b corresponding to this maximum is considered the cmc. All told, the micelle segment distribution and, as a consequence, the structure of the micelle are known at the cmc.

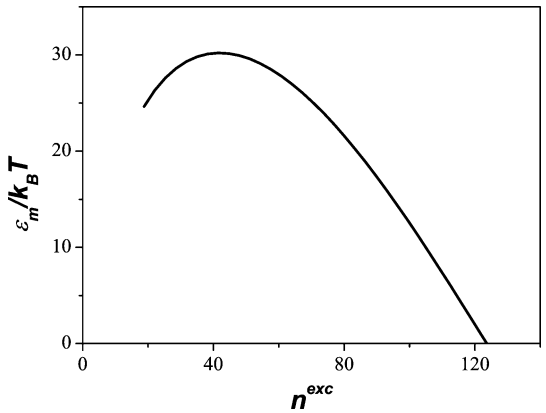

Figure 2. Translationally restricted grand potential versus aggregation number for $C_{12}E_6$ micelle in equilibrium with freely dispersed surfactants. At the maximum, $\varphi^b = 1.226 \times 10^{-4}$.

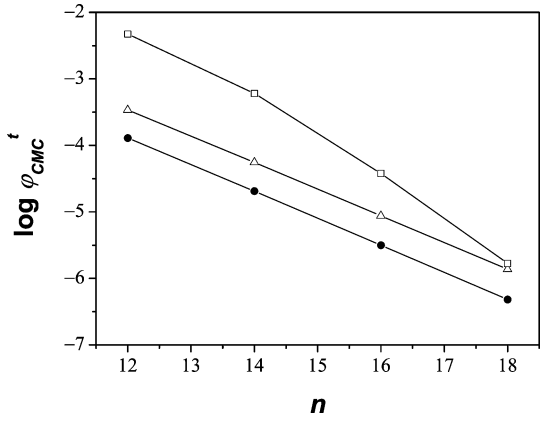

Figure 3. Effect of the tail length on the cmc for C_nE_8 solution: □, second cmc; ●, first cmc, method 1; △, first cmc, method 2. Lines are added to guide the eye.

In Figure 2 a typical example is shown for $\epsilon_m(n^{exc})$, called *stability curve*.[52] As told the maximum of this curve corresponds to the smallest micelles that are stable. The micelles that are even smaller, i.e., for which $\partial\epsilon_m/\partial n^{exc} > 0$ correspond to micelles that are macroscopically unstable. According to eq 5 the slope $-\partial\epsilon_m/\partial n^{exc}$ is inversely proportional to the relative fluctuations in micelle size (necessarily positive).[8,63] We will see this in detail below. At the top, i.e., at the cmc micelles, the fluctuations are large. Subsequently with increasing micelle size the fluctuations quickly reduce to an approximately constant value. This is in line with experimental findings. Eventually for very large values of the aggregation number n^{exc} the grand potential can become negative. This part of the curve is not experimentally accessible. It would mean that the volume fraction of micelles becomes larger than unity. Moreover at very low values of ϵ_m intermicellar interactions will become important. Below we will see that in addition the sphere-to-rod transition will prevent the system from reaching these micelle sizes.

Above we have discussed one method to define the cmc (our first definition). Formally the one that is given corresponds to the first appearance of micelles in the system. This is the usual procedure in the SCF theory for determining the cmc and it is in agreement with one of the criteria mentioned above. However, in practice this definition may give rise to micelle concentrations so low that they cannot be detected experimentally. Alternatively, one may set the cmc at the surfactant concentration at which the number of surfactants in micelles equals the number of surfactants freely dispersed in solution.[31]

The total surfactant volume fraction φ^t is composed of freely dispersed surfactants φ^b and that of micelles. If the volume of a micelle is approximated by $V_m = n^{exc}N$, where N is the number of segments in the chain, the surfactant volume fraction forming micelles is given by φ_m. As told, this latter is, for sufficiently low micelle concentration, related to the grand potential of the micelles. If we plot the total surfactant concentration versus the equilibrium concentration of free surfactant in the system (i.e., Figure 13 when only spherical micelles are considered), we see two regimes, separated by a break. We may identify the break by the experimentally accessible cmc (our second definition). For total surfactant concentration below the break, we have $\varphi^t = \varphi^b$ because φ_m is still negligible. Above the break $\varphi^t = \varphi_m$ as most of the surfactant is in micelles. At the break the volume fraction of surfactant is equally split between freely dispersed and aggregated in micelles. The surfactant concentration at the cmc obtained by this criterium is higher than that described above (see also Figure 3 below). The cmc values determined by both criteria should be considered as extreme values for the "real" (if such property exists) cmc. The experimental value will be closer to one of them depending on the accuracy of the technique used. As an example, we compare the experimental cmc for Triton X-100 (it could be approximately modeled as $C_{14}E_{10}$) obtained from spectrophotometry[64] (0.51×10^{-3} M) with that from pyrene 1:3 ratio method[65] and surface tension[66] (0.25×10^{-3} M). The ratio is 2.04. The ratio between the theoretical cmc's corresponding to $C_{14}E_8$ (cmc depends weakly on m) is 2.72. It seems to be acceptable to define a range for the cmc instead of a concrete value.

We will show below that there exist irregularities in the micelle size distribution between spherical and cylindrical (linear) micelles. Very short linear micelles have a relatively low probability. These irregularities are responsible for a jumplike change of various system properties as soon as the linear micelles appear. This occurs at a particular surfactant concentration which is known as the second cmc. Below the second cmc the strategy of the system is to increase the number of micelles at (approximately) fixed aggregation number, whereas above the second cmc the aggregation number suddenly increases and the number of micelles grows only slowly.

The existence of the second cmc can be studied using the 1D-SCF theory. Again, we highlight that this procedure only considers most likely micelles and that fluctuations will be taken into account below in the text. The identification of the second cmc starts by generating the $\epsilon_m(n^{exc})$ curve in cylindrical geometry. In this case, the object under study is an infinitely long cylindrical micelle and the quantities are obtained per unit length of the linear micelle. The entropic contributions on the micellar level, i.e., the translational as well as conformational entropy, are assumed to be negligible (we will check the latter assumption below). As a result, the equilibrium condition corresponds to the tensionless linear micelle, i.e., $\epsilon_m = 0$. The tensionless infinitely long cylindrical micelle exists at a well-defined value of the chemical potential of the surfactants.

The second step is to consider spherical micelles. Stable spherical micelles correspond to the regime of aggregation number for which $\partial\epsilon_m/\partial n^{exc} < 0$ (see Figure 2). For each stable spherical micelle size there exists a value of the surfactant chemical potential. Note that the surfactant chemical potential is an increasing function of the aggregation number. Typically there exists a chemical potential of the surfactant that corresponds to both the tensionless cylindrical micelles and spherical micelles with a well-defined aggregation number. We will concentrate on this specific value of the chemical potential of

the surfactant, μ^*. Let the grand potential of the spherical micelle that exists at μ^* be given by ϵ_m^* and the aggregation number n^{exc*}.

A sufficiently long dumbbell-like (linear) micelle typically exists at a surfactant chemical potential close to μ^*. Such a micelle can therefore be seen as having a tensionless cylindrical body and two semispherical endcaps. The ϵ_m (which will be computed below) of the dumbbell micelle should be close to ϵ_m^*, and we may use ϵ_m^* as the first estimate of the endcap (free) energy E^c. There is a one-to-one relation between μ^* and the volume fraction of surfactants freely dispersed in solution φ^{b*}. From the above it will be clear that the overall surfactant concentration is approximately given by $\varphi^{t*} = \varphi^{b*} + \exp(-\epsilon_m^*/k_BT)$, where the latter term is the volume fraction of micelles. The value of φ^{t*} may be identified as the second cmc.

In Figures 3 and 4 we present the data for the first cmc (methods 1 and 2), and the second cmc as a function of the tail length as well as the headgroup length of the nonionic surfactant system. In line with experiments the cmc is an exponentially decreasing function of the tail length, and only a weakly increasing function of the headgroup size. From a linear fit to the ln cmc versus n curve, the slope was -0.932 ± 0.003 for the first method and -0.920 ± 0.003 for the second method. By use of experimental data of such surfactants found in the literature, the slope was -0.94 ± 0.12. Therefore, the SCF predictions are quite realistic. The experimental found behavior of the cmc versus the head length was also the weak increase predicted by SCF. Szleifer et al.[31] also predicted that the cmc was only slightly dependent on the headgroup molecular architecture and decreased exponentially with the tail length. However, the slope of the ln cmc versus n curve was -0.53 ± 0.03. The second cmc is always higher than the first cmc obtained using the first criterium. It can easily happen that the second cmc is lower than the first cmc obtained using the second criterium. As the second criterium of the first cmc is probably closer to an experimentally accessible value, we conclude that it is possible that the first micelles that are observed in experiments already deviate significantly from spherical ones. This may happen for relatively large tail length and small headgroup sizes.

In passing we note that this result is in line with expectations based on the value of the surfactant packing parameter $P = v/(la_0)$, where v is the volume in the micelle occupied by a tail, l the length of the tail, and a_0 the area occupied per surfactant. Spherical micelles are expected for $P \approx 1/3$, linear micelles for $P \approx 1/2$ and bilayers for $P \approx 1$. With decreasing headgroup size, a_0 decreases and thus P increases. As a result one would expect the relative increase in stability of wormlike micelles at the expense of spherical ones when the headgroup is reduced in size. As $v \propto l$, one would not expect P to change much with increasing tail length at fixed headgroup size. Both trends can be seen in Figures 3 and 4.

2D-SCF Analysis on the Dumbbell-like Micelles. The thermodynamics of the dumbbell-like micelles can be studied because the partition function of the system is accurately available through the 2D-SCF calculations. The resulting ϵ_m-(n^{exc}) curves by using this theory in cylindrical geometry for all the surfactants mentioned above follow the same pattern: there is an oscillatory behavior with an amplitude that decreases exponentially until it reaches a limiting constant value. This limiting value is identified by the endcap free energy E^c. As an example, the (stability) curve for the surfactant $C_{12}E_6$ is presented in Figure 5. Instead of the aggregation number, a quantity that represents the length of the body of the dumbbell-like micelle is used on the x axis. The conversion between the aggregation number and the length is possible when the number of surfactants per unit length n_0^{exc} is known. This quantity is accurately calculated from the tensionless cylindrical micelle as computed in the 1D-SCF model discussed above

$$L = \frac{n^{exc}}{n_o^{exc}} \tag{6}$$

As with all other length scales, the length of the linear micelle L is normalized with the size l of a lattice site.

In Figure 6 we plot $\ln|\epsilon_m - E^c|$ versus L for each maximum and minimum in the $\epsilon_m(L)$ curve. The linear behavior proves

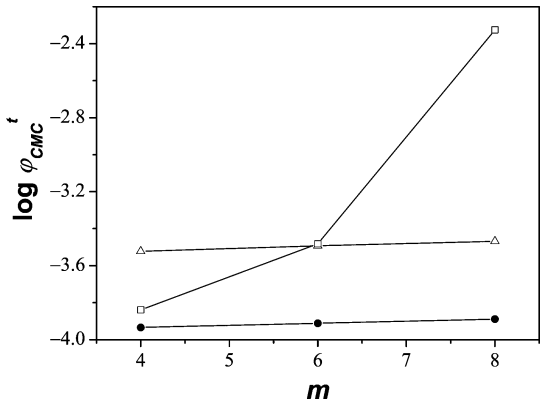

Figure 4. Effect of the head length on the cmc for $C_{12}E_m$ solution: □, second cmc; ●, first cmc, method 1; △, first cmc, method 2.

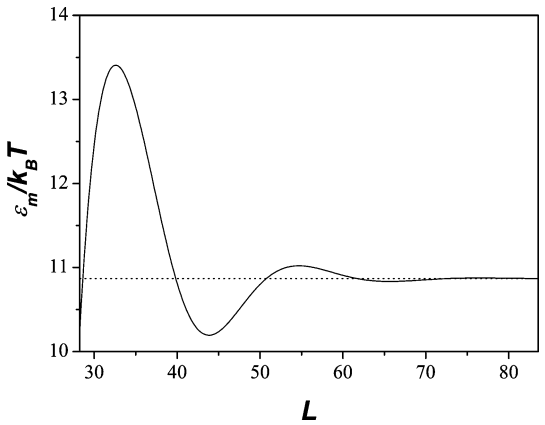

Figure 5. Translationally restricted grand potential ϵ_m versus the length L of the dumbbell-like micelles from 2D-SCF calculations for $C_{12}E_6$ surfactants.

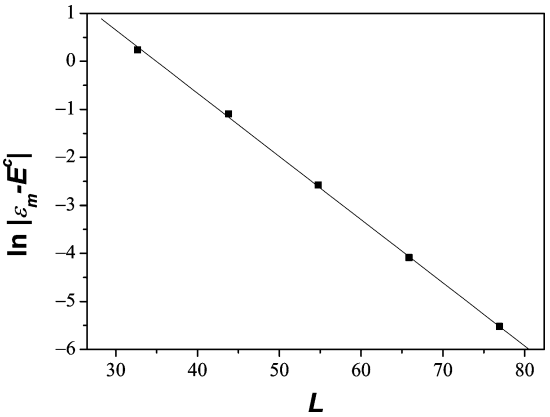

Figure 6. The logarithm of the "amplitude" A of the extrema in ϵ_m-(n^{exc}) curve versus L for $C_{12}E_6$ solution.

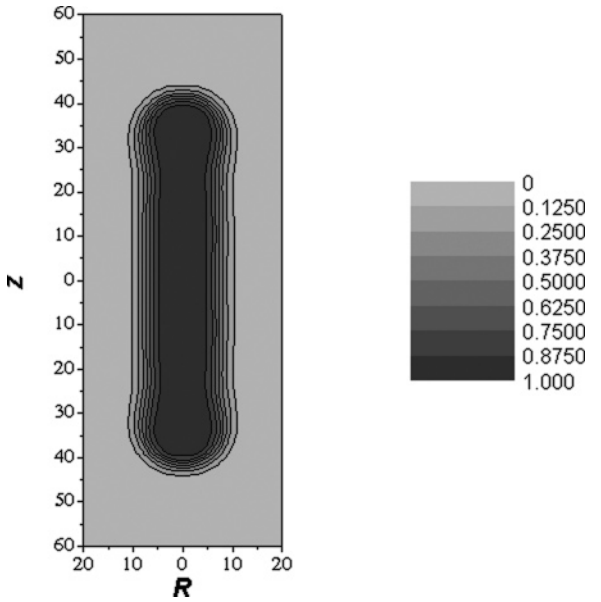

Figure 7. 2D "equal density" contour plot of the overall surfactant volume fraction profile for a linear micelle composed of $C_{12}E_6$ surfactants at $\varphi^b = 1.6074 \times 10^{-4}$.

the exponential decrease of the amplitude mentioned above. By defining the amplitude as $A = |\epsilon_m - E^c|$, we can conclude that the data are consistent with

$$A(L) = A_0 \exp\left(-\frac{L}{\xi}\right) \tag{7}$$

which defines the decay length ξ and A_0 which is the amplitude extrapolated to $L = 0$. The latter quantity has no direct physical meaning.

A contour plot representing the volume fraction profiles in gray scaling for a finite cylindrical micelle is shown in Figure 7. The shape resembles a dumbbell. The structure has many features in common with simple micelles. The inside of the object (core) is mostly composed of surfactant tails. The headgroups are on the outside forming a hydrophilic corona. From the contour plots it is easily seen that the ends of the micelle have a slightly larger radius than the body. This effect is not easily measured experimentally but may be understood from packing considerations. In the terminal regions there is a local spherical topology. In the center of the sphere there is little space. Only a few chains have to reach the center in order to fill this region with chains. The remainder of the chains do not have to stretch as much and therefore can pack with less entropy loss. As a result the core of the micelle can continue to grow slightly more than in the cylindrical geometry. Apart from this more obvious feature there are several less obvious aspects to be mentioned. One of them is the appearance of a neck. Going from the cap to the body there appears a region with a minimum in the radius. Below we will argue that the existence of the neck causes the reduced probability to find these short linear micelles.

Returning to Figure 5, by using the micelle stability criterium mentioned before, the first stable dumbbell micelle corresponds to the first maximum in the stability curve $\epsilon_m(n^{exc})$. By decreasing the aggregation number there is a regime with a positive slope $\partial\epsilon_m(n^{exc})/\partial n^{exc} > 0$. This corresponds to unstable micelle sizes. By decreasing the aggregation number even further, i.e., $L < 30$ (not shown), we will reenter a region of stable spherical micelles. In the SCF model we typically concentrate on most-likely micelles. As mentioned above the slope $\partial\epsilon_m(n^{exc})/\partial n^{exc}$ is inversely proportional to the fluctuations in micelle sizes. The fluctuation picture of micellar solutions is of course more accurate than a picture based on most-likely micelles. We therefore do not expect the total absence of intermediate micelle sizes but rather envision that these intermediate micelles just have a low probability. Below we will elaborate on this in more detail. In line with Porte et al.'s definition on the second cmc,[30] we can establish this value at the situation when oscillations finish. At this point only the endcap energy contributes to the free energy. The calculations confirm that the surfactant chemical potential at this point is equal to μ^*.

With increasing the aggregation number such that the length $L > 35$ (see Figure 5), we alternatingly enter sizes of linear micelles that are stable and unstable. Besides the consequences with respect to the micelle length distribution as qualitatively discussed above, there exists an alternative way to discuss these results. One can think of $\Delta\epsilon(L) \equiv \epsilon_m(L) - \epsilon_m(\infty)$ as an interaction curve between the two endcaps. This interaction must be mediated by the surfactants in the body. Indeed, if these surfactants are not perturbed in their conformation, there is no way they can "transport" the knowledge of their proximity to the endcaps. For very large micelles the two endcaps do not see each other and the interaction energy remains zero. Only the endcap energy contributes to the free energy, because the body is tensionless (the surfactants are distributed in the body in an optimal way). However, by shorting the micelle, the surfactants distribute in more or less favorable ways (minimum or maximum in the energy curve) and the endcaps feel each other closer and closer. Therefore, for smaller values of L, the interaction energy changes oscillatory with increasing amplitude, similar to structural forces. For example the relatively large attraction found when the length of the micelle $L \approx 30$ is caused by the overlap of the neck regions. May et al.[37] also found a damped oscillatory behavior of the packing free energy of a linear micelle as a function of the aggregation number. However, they did not attribute special physical significance to these oscillations as they were supposed to be associated to one of the simplifications in the model: their neglect of the tilt degree of freedom. The SCF results prove that this last argument is not valid because the tilt degree of freedom is explicitly included in the theory and significant oscillations are nevertheless observed.

For sufficiently large aggregation number $\epsilon_m(n^{exc})$ becomes independent of n^{exc}. From a fluctuation point of view, we will show that this indicates that the relative fluctuations diverge. This means that we expect large variations in lengths. Taking into account that the amount of surfactants in the system is fixed, it will be shown that the size distribution becomes exponential. This means that the conservation of molecules damps the fluctuations in micelle size.

The explicit coexistence between cylindrical and spherical micelles would require a computation wherein in one and the same coordinate system a spherical micelle coexists with a dumbbell-like one. Although this is in principle possible, we have not attempted such a calculation. The coexistence of spheres with cylinders is thus deduced from a thermodynamic analysis of the system alone. As an example, the stability curve of the surfactant $C_{12}E_4$ and the corresponding surfactant chemical potential curve are presented in Figure 8. Throughout the stability curve, $\epsilon_m(n^{exc})$, there exist stable solutions of micelles that correspond to the same chemical potential. This means that at such a chemical potential dumbbell micelles of different size and, also, the corresponding stable spherical

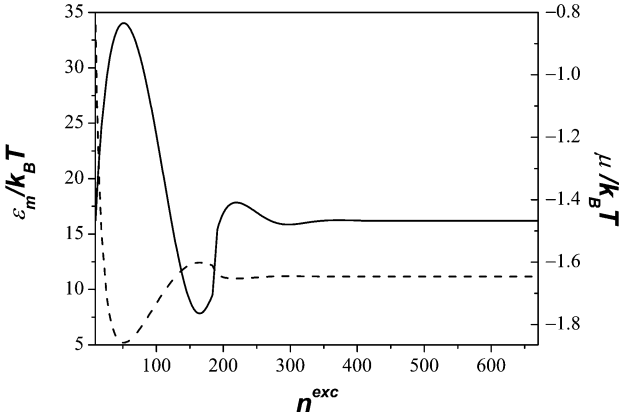

Figure 8. The translationally restricted grand potential $\epsilon_m(n^{exc})$ (solid line) and the surfactant chemical potential (dash line) of micelles composed of $C_{12}E_4$ surfactants as a function of the aggregation number n^{exc}.

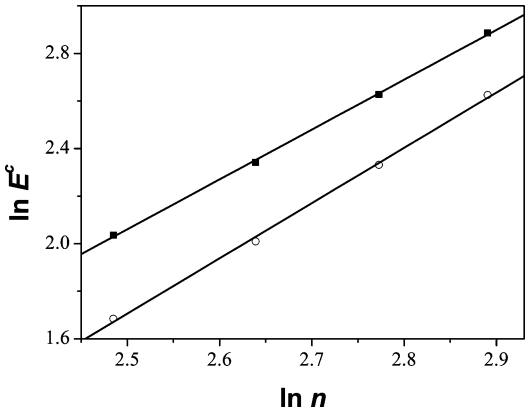

Figure 9. Endcap energy from 2D-SCF (■) and 1D-SCF (○) as a function of the tail length for C_nE_8 solution.

micelle (low n^{exc} region) coexist. The volume fraction of spherical micelles and of the various dumbbells are proportional to $\exp(-\epsilon_m/k_BT)$. Inspection of Figure 8 shows that the volume fraction of spherical micelles will exceed the volume fraction of the various dumbbells. Further on in the paper, we generate the corresponding micelle size distribution.

Similar 2D-SCF calculations have been carried out for various members of the C_nE_m nonionic family to investigate the influence of the tail length (n), the head length (m), and the total number of segments in the chain (N). The endcap energy obtained through the 2D-SCF analysis has been compared with that from 1D-SCF for the different chains in Figure 9. It is found that the endcap energy from the 1D model underestimates the true value systematically. This difference in the endcap energy is of course anticipated. In fact the difference is much less than one would expect intuitively. As a result we can use the 1D model, which is an order of magnitude more efficient CPU-wise, to find reasonable predictions for the endcap energy. As shown in Figure 9 the endcap energy increases approximately quadratic with the tail length, i.e., $E^c \propto n^\alpha$ with $\alpha = 2.10 \pm 0.04$. As the radius of the micelle is in first order proportional to the tail length, we thus find that the endcap energy scales roughly quadratic with the radius of the micelle (core). We have not found enough experimental data on endcap energies of linear micelles of nonionic surfactants to compare with our theoretical results. Kwon et al.[43] reported a value of 21.6 k_BT at 15 °C for the $C_{12}E_5$ surfactant. This value was obtained from SLS measurements of the length of the micelle that were conversed to the endcap energy value by using the approximation that the

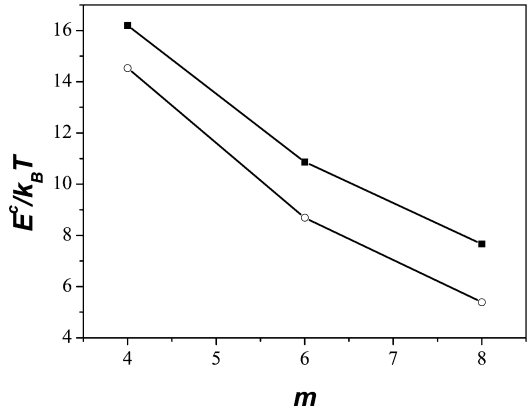

Figure 10. Endcap energy from 2D-SCF (■) and 1D-SCF (○) as a function of the head length for $C_{12}E_m$ solution.

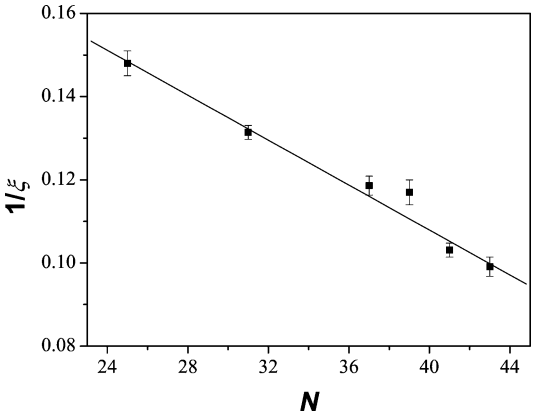

Figure 11. The inverse of the decay length, i.e., $1/\xi$ as a function of the length of the surfactant $N = n + 3m + 1$ for linear micelles composed of C_nE_m surfactants.

mean length is exponentially dependent on the scission energy. Our results also show that the endcap energy E^c diminishes by increasing m (Figure 10). With increasing headgroup size we reduce the core radius somewhat which results in a reduction of the endcap energy. The lower the endcap energy, the more favorable the spherical micelle. Indeed, with increasing headgroup size we expect spherical micelles to be thermodynamically increasingly stable.

The effect of the chain characteristics on the decay length ξ as defined in eq 7 was also analyzed. It was found that, $1/\xi$ diminishes linearly with n, m, and N. This last relation is presented in Figure 11. It is not obvious why the decay length increases with increasing N or, to pose it differently, why the oscillation dies out quicker for shorter chains than for longer ones. One may argue that conformational distortions away from the local normal will cost some energy. The more easy it is (less energy) to form nonnormal conformations, the easier it is to adjust to the thickness variations (ξ is small). If nonnormal conformations are effectively forbidden, it is expected that the oscillation will persist (ξ is large). From this argument we thus may conclude that apparently the shorter surfactants may accommodate nonnormal conformations better than the longer ones.

The wavelength of the oscillation (λ_d) in the stability curve, i.e., $\epsilon_m(n^{exc})$, this is, the number of surfactants needed to go from one maximum to the following one, increases linearly with the tail length n as $\lambda_d = 4.7 + 0.53n$. This is not unexpected. It must be true that the local thickness variations in the cylindrical body of the micelles propagate along the cylindrical micelle through the conformational properties of the surfactants.

As the influence of the local conformations of surfactants cannot be felt further than the length of the surfactants, it is quite natural that the surfactant length sets the length scale of the oscillations.

Bending and Stretching Modulus of Cylindrical Micelles. In this section we elaborate on different mechanical properties of the linear micelles: stiffness and extendability.

In the SCF analysis of the linear micelles, it was assumed that they did not have significant contributions from entropic origin on the micellar level. We can identify two potential contributions: (1) translational entropy and (2) conformational entropy.

Let us first discuss the translational entropy of the linear micelle. Similarly as spherical micelles, the linear micelles will have a finite amount of translational entropy. For dilute solutions the value is proportional to the logarithm of the volume fraction of micelles (typically of order 10 k_B). For very long linear micelles, the translational entropy can safely be ignored: per unit length this entropic contribution is negligible (typically of order 0.2 k_B).

To estimate the conformational entropy it is necessary to know the persistence length l_p, that is, the length along the contour of the micelle over which the correlation of directional orientation is reduced by a factor e. It is established that if the length of the micelle is smaller than l_p, the micelle behaves nearly as a rod, whereas a flexible cylindrical micelle is found in the opposite case. In first order, the cylinder has a conformational entropy contribution to the grand potential per unit length of order k_BT per persistence length. If the persistence length is short, i.e., $l_p \approx 1$, this may contribute significantly to the grand potential of the cylindrical micelle per unit length. However when $l_p \gg 1$, the conformational contribution per unit length equals $k_BT/l_p \approx 0$. This latter scenario is expected to be true, but this should be checked.

Here we follow the procedure of Lauw et al.[58] to evaluate the persistence length of linear micelles. In this procedure one considers linear micelles that are homogeneously curved into a torus with radius R. As the torus has no ends, it can be formed from a piece of the (tensionless) body of the linear micelles. We can interpret the grand potential of the torus-shaped micelle as the curvature energy stored in the torus. The inverse of the radius is the curvature $J = 1/R$ and the grand potential of the torus can be parametrized for low values of the curvature with the Helfrich formula

$$\epsilon_t(J) = 2\pi R\left(\frac{1}{2}k_c J^2\right) = \pi J k_c \tag{8}$$

where the bending modulus k_c is a measure for the stiffness of the linear micelle and has units $k_BT\ l$. Taking the Ansatz that the persistence length l_p corresponds to the size of torus with curvature energy of $1k_BT$, we find

$$l_p = \frac{k_c}{k_BT} \tag{9}$$

The persistence lengths obtained for the different surfactant chains are presented in Table 1. The main lengths defined in this paper are also included in the table (decay length, wavelength (λ_d)).

In a previous study,[58] the persistence was found to increase as a power law with the tail length of the surfactant. In line with this we report $l_p \sim n^\beta$, where $\beta = 2.29 \pm 0.05$. Also in line with previous studies we find that the persistence length is independent of the headgroup length (at fixed (n)). More importantly, we conclude that the persistence length of the linear micelles is much larger than unity and the typical Ansatz that the conformational entropy of the wormlike micelles can be ignored is reasonable in all cases.

TABLE 1: Collection of Various Characteristics of Linear Micelles for Different C_nE_m Surfactants[a]

	$C_{12}E_4$	$C_{12}E_6$	$C_{12}E_8$	$C_{14}E_8$	$C_{16}E_8$	$C_{18}E_8$
l_p	49.11	49.86	49.20	71.44	96.75	124.34
ξ	6.76	7.61	8.43	8.55	9.70	10.09
λ_d	22.73	22.13	22.21	23.96	26.49	28.40
n_o^{exc}	6.69	5.47	4.82	5.27	5.71	6.14
k_L	6.63	6.87	6.35	7.82	9.16	10.42

[a] The lengths are expressed in units of the size of a lattice site (0.2 nm) and the stretching modulus in k_BT per unit length.

Another interesting mechanical property of the linear micelles is their extendibility, i.e., the energy necessary to slightly stretch the rod at a constant surfactant concentration. In line with studies on membrane stretching,[67] we can define the stretching modulus for linear micelles (k_L) from the data corresponding to infinitely long cylindrical micelles. Small fluctuations of the micelle length at equilibrium (tensionless cylinder with number of molecules per unit length n_o^{exc}) give rise to a change in the restricted grand potential per unit length. Therefore, it is reasonable to define the stretching modulus as

$$k_L = -\left(\frac{\partial \epsilon_m{}^L}{\partial \ln n_L{}^{exc}}\right)_{no}^{exc} \tag{10}$$

where L in $\epsilon_m{}^L$ and $n_L{}^{exc}$ indicates that they are quantities per unit length (as obtained from 1D-SCF in cylindrical geometry). The stretching modulus of linear micelles has units of energy per unit length. The n_o^{exc} and k_L values calculated for the different surfactants are presented in Table 1. It can be seen than they both increase linearly with the surfactant tail length and remain almost constant with the surfactant head length.

Micelle Size Distribution. In general, we should expect the coexistence of micelles of different size at certain surfactant chemical potential. A function to calculate the distribution of micelle size for spherical micelles from SCF data has been proposed elsewhere.[68] This function, named as micelle grand potential ($\Omega_m(n^{exc})$), was defined by taking into account fluctuations in micelle sizes. At fixed values of the chemical potentials (μ_i), T, and P, such a function should have a minimum at the most likely micelle size. Very close to this minimum, in first approximation, $\Omega_m(n^{exc})$ is assumed to be a quadratic function of the micellar size

$$\Omega_m(n^{exc}) = \Omega_m(\langle n^{exc}\rangle) + K_{n^{exc}}(n^{exc} - \langle n^{exc}\rangle)^2 \tag{11}$$

where $\Omega_m(\langle n^{exc}\rangle)$ is the quantity that is computed in the SCF calculations ($\epsilon_m(\langle n^{exc}\rangle)$) and $\langle n^{exc}\rangle$ is the aggregation number of the most frequent micelle.

The size distribution is Gaussian (at least around the minimum)

$$\varphi_m(n^{exc}) = \exp\left(-\frac{\Omega_m(n^{exc})}{k_BT}\right) = \exp\left(-\frac{\epsilon_m(\langle n^{exc}\rangle)}{k_BT}\right)\exp\left(-\frac{(n^{exc} - \langle n^{exc}\rangle)^2}{2\sigma_n{}^{exc}}\right) \tag{12}$$

and the width of the distribution is given by

$$\sigma_{n^{exc}}{}^2 = -k_B T \frac{\langle n^{exc}\rangle}{\left(\frac{\partial \epsilon_m}{\partial n^{exc}}\right)_{\langle n^{exc}\rangle}} \quad (13)$$

From SCF calculations, one obtains $\langle n^{exc}\rangle$, $\epsilon_m(\langle n^{exc}\rangle)$, and $(\partial\epsilon_m/\partial n^{exc})_{\langle n^{exc}\rangle}$, and the size distribution can be generated.

In this paper, we propose a more general omega function for calculating the micelle size distribution. As told before, at a certain surfactant chemical potential ($\mu^{\ddagger}$) SCF calculations provide the aggregation number of the most frequent micelle, i.e., $\langle n^{exc}\rangle$, and the corresponding translationally restricted grand potential ($\epsilon_m(\langle n^{exc}\rangle)$). By considering the fluctuations in size, we define the following function

$$\Omega_m(n^{exc}) = \epsilon_m(n^{exc}) + n^{exc}[\mu(n^{exc}) - \mu(\langle n^{exc}\rangle)] \quad (14)$$

where $\mu(\langle n^{exc}\rangle) = \mu^{\ddagger}$. It can be shown from the data that the solvent contribution is negligible.

Then, the size distribution at certain $\mu^{\ddagger}$ is given by

$$\varphi_m(n^{exc}) = \exp\left(-\frac{\Omega_m(n^{exc})}{k_B T}\right) \quad (15)$$

In the Appendix, we demonstrate that this function becomes Gaussian (as predicted elsewhere[68]) when small fluctuations are considered. This takes place, e.g., when only spherical micelles are present in the system. However, at $\mu^{\ddagger}$ values at which spherical and dumbbell-like micelles are coexisting, the size distribution presents different features and deviates strongly from the Gaussian. In Figure 12 we show the micelle size distribution at different $\mu^{\ddagger}$ values for $C_{12}E_4$ surfactant.

The dash−dot line corresponds to a chemical potential at which only spherical micelles appear in the system. We can see that it is a Gaussian distribution. When dumbbells appear, different features can be observed. A sharp peak corresponding to the most likely spherical micelle size is still present. However, new findings corresponding to the contribution of finite dumbbells should be highlighted. The lower probability found at certain micelle aggregation numbers (they are better shown in Figure 12) can be explained by means of the stability curve (Figure 8): the unstable micelle regions in such a curve are translated to low probability regions in the size distribution curve. Finally, in Figure 12, we also show that the distribution becomes exponential for large rods, as predicted by other authors. Therefore, besides predicting universal behaviors for the micelle size distribution, SCF theory allows us to realize the role of the finite rods on the micelle size distribution.

The total volume fraction of micelles at certain $\mu^{\ddagger}$ can be calculated from the micelle size distribution

$$\varphi_m^{total} = \int_0^{\infty} \varphi_m(n^{exc})\, dn^{exc} \quad (16)$$

Then, we can plot the total surfactant concentration versus the bulk surfactant concentration to get information on the micelle shape transition. In Figure 13 we compare the results for two type of surfactants, $C_{12}E_4$ (circle) and $C_{12}E_4$ (square), when dumbbells are taken into account (solid symbol) and when they are neglected (open symbol). All data are obtained by including the micelle size distribution.

On one hand, the deviation from the dot line allows us to predict the first cmc (short arrows). On the other hand, the deviation of the solid scattered line from the open scattered line gives information on the second cmc (long arrows). The effect

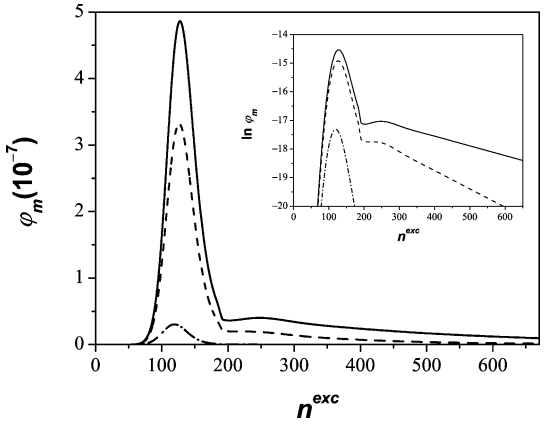

Figure 12. Micelle size distribution for micelles composed of $C_{12}E_4$ surfactants. Inset in logarithm scale. At $\mu^{\ddagger}/k_BT = -1.64937$ ($\varphi^b = 1.4401 \times 10^{-4}$ (solid line), -1.65238 ($\varphi^b = 1.4357 \times 10^{-4}$ (dash line), -1.67189 ($\varphi^b = 1.4079 \times 10^{-4}$ (dash−dot line).

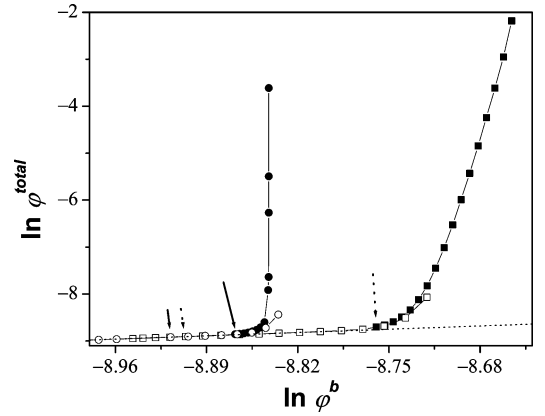

Figure 13. Total surfactant concentration versus bulk surfactant concentration for micelles composed of $C_{12}E_4$ surfactants (circle) and $C_{12}E_8$ surfactants (square). Dumbbells are taken into account (solid symbol), dumbbells are neglected (open symbol). First cmc: $C_{12}E_4$ (short solid arrow) and $C_{12}E_8$ (short dot arrow). Second cmc: $C_{12}E_4$ (long solid arrow) and $C_{12}E_8$ (long dot arrow). Dotted line for $\varphi^b = \varphi^{total}$.

of the surfactant characteristics on the transition behavior predicted by using the size distribution is also shown in Figure 13. The size of the headgroup is not as important for the first cmc as for the second cmc. From these data φ^t(first cmc) = 1.34×10^{-4} and 1.36×10^{-4} for $C_{12}E_4$, and $C_{12}E_8$, respectively. And φ^t(second cmc) = 1.42×10^{-4} and 1.66×10^{-4} for $C_{12}E_4$ and $C_{12}E_8$, respectively. When these values are compared with those obtained without including fluctuations in size (see figure) differences are found, as not only the most likely micelles are considered for calculating the total surfactant amount forming micelles.

From the micelle size distribution at certain $\mu^{\ddagger}$, we can calculate the average aggregation number ($\overline{n^{exc}}$), and the fluctuation in size ($\sigma_n{}^{exc}$) as

$$\overline{n^{exc}} = \frac{\int_0^{\infty} n^{exc}\varphi_m(n^{exc})\, dn^{exc}}{\int_0^{\infty} \varphi_m(n^{exc})\, dn^{exc}} \quad (17)$$

and $\sigma_{n^{exc}}{}^2 = \overline{(n^{exc})^2} - (\overline{n^{exc}})^2$ with

$$\overline{(n^{exc})^2} = \frac{\int_0^\infty (n^{exc})^2 \varphi_m(n^{exc})\, dn^{exc}}{\int_0^\infty \varphi_m(n^{exc})\, dn^{exc}} \quad (18)$$

These values at different total concentrations are shown in Table 2. In agreement with other authors,[69] micellar size increases monotonically with increasing surfactant concentration. Size fluctuation results are explained by observing the curves in Figure 12. As discussed, finite rods also contribute to the micelle size distribution.

If we plot $\log(\overline{n^{exc}})$ as a function of $\log(\varphi_m^{total})$ (see Figure 14), we see that above a certain surfactant concentration the average micelle size scales as $\overline{n^{exc}} \simeq (\varphi_m^{total})^{1/2}$ as found in the literature.[69]

Conclusions

From the above we can conclude that the SCF theory may be used to investigate the sphere-to-cylinder transition in micellar systems. As in the simulation route, the SCF theory provides detailed information on the micelle structures. However, SCF theory also gives detailed insight in the thermodynamics on the micellar level of the system. All this allowed us to consider the dumbbell shape of the cylindrical micelles near the second cmc. Largely in line with experimental findings, the theory predicts the coexistence of micelles of different size and shape and allows us to generate the micelle size distribution. We have shown that this micelle size distribution can be nonmonotonic due to the presence of very short dumbbell-like micelles with a relatively low probability. Within the same parameter setting it is possible to find not only the endcap energy but also other mechanical properties such as the persistence length and the stretching modulus of the corresponding uniaxial micelles. Using these parameters it is possible to construct a mesoscopic model for wormlike micellar solutions. Our analysis has confirmed the hypothesis that the endcap energy can be estimated in first order by a simple 1D-SCF analysis. This is conceptually interesting as it opens the possibility to use the SCF theory to estimate the endcap energies of more complex micellar systems; e.g., it may be used to predict the effect of additives (solubilization) on the endcap energy, study the endcap energy of linear micelles composed of charged surfactant, or evaluate this property for surfactant mixtures. Finally, the fact that the hydrophobic moiety of the surfactant influences the endcap energy has been quantitatively confirmed by finding that the endcap energy increases approximately quadratic with the tail length.

Acknowledgment. This work is based on a postdoctoral fellowship supported by the Spanish "Ministerio de Educacion, Cultura y Deporte". Ana Belén Jódar-Reyes would like to thank the Laboratory of Physical Chemistry and Colloid Science of Wageningen University in The Netherlands for hosting her for the duration of this project. Finally, the Consejeria de Infraestructuras y Desarrollo Tecnológico, Junta de Extremadura is also acknowledged.

TABLE 2: Average Aggregation Number and Size Fluctuations for Micelles of $C_{12}E_4$ at Different Surfactant Concentrations

φ_m^{total} (10^{-5})	0.15	0.23	0.35	0.54	0.84	1.32	2.16	4.00
$\overline{n^{exc}}$	124	126	129	133	139	149	173	258
$\sigma_{n^{exc}}$	25	27	31	38	47	68	113	245

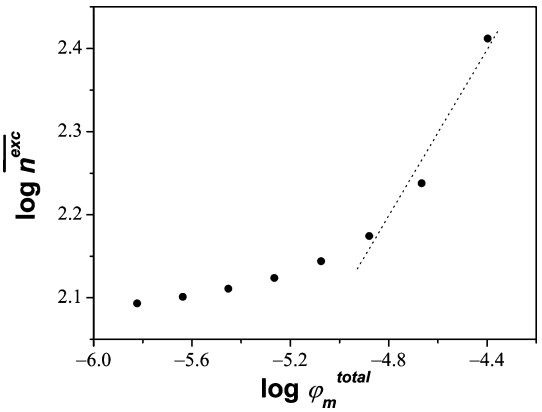

Figure 14. Average micelle size as a function of the total surfactant concentration in micelles for $C_{12}E_4$ surfactant. The dotted line has a slope of 1/2.

Appendix

The goal of this appendix is to demonstrate that the $\Omega_m(n^{exc})$ function defined in eq 11 becomes a quadratic function of the micelle size when small fluctuations are considered.

The start is to introduce Taylor expansions for $\epsilon_m(n^{exc})$ and $\mu(n^{exc})$ around the $\langle n^{exc}\rangle$

$$\epsilon_m(n^{exc}) = \epsilon_m(\langle n^{exc}\rangle) + \left(\frac{\partial \epsilon_m}{\partial n^{exc}}\right)_{\langle n^{exc}\rangle} (n^{exc} - \langle n^{exc}\rangle) + \frac{1}{2}\left(\frac{\partial^2 \epsilon_m}{\partial_n^{exc2}}\right)_{\langle n^{exc}\rangle} (n^{exc} - \langle n^{exc}\rangle)^2 \quad (19)$$

$$\mu(n^{exc}) = \mu(\langle n^{exc}\rangle) + \left(\frac{\partial \mu}{\partial n^{exc}}\right)_{\langle n^{exc}\rangle} (n^{exc} - \langle n^{exc}\rangle) + \frac{1}{2}\left(\frac{\partial^2 \mu}{\partial_n^{exc2}}\right)_{\langle n^{exc}\rangle} (n^{exc} - \langle n^{exc}\rangle)^2 \quad (20)$$

From eq 4 we know

$$\left(\frac{\partial \mu}{\partial n^{exc}}\right)_{\langle n^{exc}\rangle} = -\frac{1}{\langle n^{exc}\rangle}\left(\frac{\partial \epsilon_m}{\partial n^{exc}}\right)_{\langle n^{exc}\rangle} \quad (21)$$

and

$$\left(\frac{\partial^2 \mu}{\partial_n^{exc2}}\right)_{\langle n^{exc}\rangle} = \frac{1}{\langle n^{exc}\rangle^2}\left(\frac{\partial \epsilon_m}{\partial n^{exc}}\right)_{\langle n^{exc}\rangle} - \frac{1}{\langle n^{exc}\rangle}\left(\frac{\partial^2 \epsilon_m}{\partial_n^{exc2}}\right)_{\langle n^{exc}\rangle} \quad (22)$$

In setting eqs 21 and 22 into eq 20, and using eq 11, we have

$$\Omega_m(n^{exc}) = \epsilon_m(\langle n^{exc}\rangle) + \left(\frac{\partial \epsilon_m}{\partial n^{exc}}\right)_{\langle n^{exc}\rangle} A + \left(\frac{\partial^2 \epsilon_m}{\partial_n^{exc2}}\right)_{\langle n^{exc}\rangle} B \quad (23)$$

with

$$A \equiv (n^{exc} - \langle n^{exc}\rangle) - \frac{n^{exc}}{\langle n^{exc}\rangle}(n^{exc} - \langle n^{exc}\rangle) + \frac{1}{2}\frac{n^{exc}}{\langle n^{exc}\rangle^2}(n^{exc} - \langle n^{exc}\rangle)^2 = -\frac{(n^{exc} - \langle n^{exc}\rangle)^2}{2\langle n^{exc}\rangle} + \frac{(n^{exc} - \langle n^{exc}\rangle)^3}{2\langle n^{exc}\rangle^2}$$

$$B \equiv \frac{1}{2}(n^{exc} - \langle n^{exc}\rangle)^2 - \frac{1}{2}\frac{n^{exc}}{\langle n^{exc}\rangle}(n^{exc} - \langle n^{exc}\rangle)^2 = -\frac{(n^{exc} - \langle n^{exc}\rangle)^3}{2\langle n^{exc}\rangle}$$

If only small fluctuations in size are considered, we can neglect the term $(n^{exc} - \langle n^{exc}\rangle)^3$, and eq 23 becomes

$$\Omega_m(n^{exc}) = \epsilon_m(\langle n^{exc}\rangle) - \frac{1}{\langle n^{exc}\rangle}\left(\frac{\partial \epsilon_m}{\partial n^{exc}}\right)_{\langle n^{exc}\rangle}\frac{(n^{exc} - \langle n^{exc}\rangle)^2}{2} \quad (24)$$

This is a quadratic function of the micelle size.

The corresponding micelle size distribution (as given by eq 15) is a Gaussian function whose width is given by

$$\sigma_{n^{exc}}{}^2 = -k_B T \frac{\langle n^{exc}\rangle}{\left(\frac{\partial \epsilon_m}{\partial n^{exc}}\right)_{\langle n^{exc}\rangle}} \quad (25)$$

Therefore, this new definition of $\Omega_m(n^{exc})$ is consistent with the fact that $-k_m T \partial n^{exc}/\partial \epsilon_m$ is related to the relative fluctuations in the micellar aggregation number (see eq 5).

The $\Omega_m(n^{exc})$ function as defined in eq 11 is also of use for systems that have a non-Gaussian size distribution, e.g., for systems with linear micelles.

References and Notes

(1) Debye, P.; Anacker, E. W. *J. Phys. Colloid Chem.* **1951**, *55*, 644.
(2) Stigter, D. *J. Phys. Chem.* **1966**, *70*, 1323.
(3) Herrmann, K. W. *J. Phys. Chem.* **1964**, *68*, 1540.
(4) Hayashi, S.; Ikeda, S. *J. Phys. Chem.* **1981**, *84*, 744.
(5) Ikeda, S.; Hayashi, S.; Imae, T. *J. Phys. Chem.* **1981**, *85*, 106.
(6) Kato, T.; Kanada, M.; Seimiya, T. *J. Colloid Interface Sci.* **1996**, *181*, 149.
(7) *Physics of Amphiphiles*: *Micelles, Vesicles and Microemulsions*; Degiorgio, V., Corti, M., Eds.; North-Holland: Amsterdam, 1985.
(8) Majhi, P. R.; Dubin, P. L.; Feng, X.; Guo, X.; Leermakers, F. A. M.; Tribet C. *J. Phys. Chem. B* **2004**, *108*, 5980.
(9) Molina-Bolıvar, J. A.; Aguiar, J.; Peula-Garcıa, J. M.; Carnero Ruiz, C.
(10) *J. Phys. Chem. B* **2004**, *108*, 12813.
(11) Khan, A.; Kaplun, A.; Talmon, Y.; Hellsten, M. *J. Colloid Interface Sci.* **1996**, *181*, 191.
(12) Bernheim-Groswasser, A.; Zana, R.; Talmon, Y. *J. Phys. Chem. B* **2000**, *104*, 4005.
(13) Haile, J. M.; O'Connell, J. P. *J. Phys. Chem.* **1986**, *90*, 1875.
(14) Jönsson, B.; Edholm, O.; Teleman, O. *J. Phys. Chem.* **1986**, *85*, 2259.
(15) Watanabe, K.; Ferrario, M.; Klein, M. L *J. Phys. Chem.* **1988**, *92*, 819.
(16) Smit, B.; Hilbers, P. A. J.; Esselink, K.; Rupert, L. A. M.; van Os, N. M.; Schlijper, A. G. *Nature* **1990**, *348*, 624.
(17) Smit, B.; Hilbers, P. A. J.; Esselink, K.; Rupert, L. A. M.; van Os, N. M.; Schlijper, A. G. *J. Phys. Chem.* **1991**, *95*, 6361.
(18) Boek, E. S.; Den Otter, W. K.; Briels, W. J.; Iakovlev D. *Math. Phys. Eng. Sci.* **2004**, *362*, 1625.
(19) Den Otter, W. K.; Shkulipa, S. A.; Briels, W. J. *J. Chem. Phys.* **2003**, *119*, 2363.
(20) Ben-Shaul, A.; Gelbart, W. M. In *Micelles, membranes, Microemulsions and Monolayers*; Gelbart, W. M., Ben-Shaul, A., Roux, D., Eds.; Springer: Berlin, 1994; Chapter 1.
(21) Hoeve, C. A. T.; Benson, G. C. *J. Phys. Chem.* **1957**, *61*, 1149.
(22) Aranow, R. H. *J. Phys. Chem.* **1963**, *67*, 556.
(23) Poland, D. C.; Scheraga, H. A. *J. Phys. Chem.* **1965**, *69*, 2431.
(24) Hall, D. G.; Pethica, B. A. In *Nonionic surfactants*; Schick, M. J., Ed.; Dekker: New York, 1967; Vol. 1, Chapter 16.
(25) Hill, T. L. *Thermodynamics of small systems*; Benjamin: New York, 1963, 1964; Vols. 1 and 2.
(26) Corkill, J. M.; Goodman, J. F.; Harrold, S. P. *Trans. Faraday Soc.* **1964**, *60*, 202.
(27) Vold, M. J. *J. Colloid Sci.* **1950**, *5*, 506.
(28) Stainsby, G.; Alexander, A. E. *Trans. Faraday Soc.* **1950**, *46*, 587.
(29) Matijevi 'c, B. A.; Pethica, B. A. *Trans. Faraday Soc.* **1958**, *54*, 587.
(30) Porte, G.; Appell, J. *J. Phys. Chem.* **1981**, *85*, 2511.
(31) Porte, G.; Poggi, Y.; Appell, J.; Maret, G. *J. Phys. Chem.* **1984**, *88*, 5713.
(32) Guerin, C. B. E.; Szleifer, I. *Langmuir* **1999**, *15*, 7901.
(33) Leermakers, F. A. M.; Scheutjens, J. M. H. M.; Lyklema, J. *Biophys. Chem.* **1983**, *18*, 353.
(34) Hall, D. G. In *Nonionic surfactants*; Schick, M. J., Ed.; Marcel Dekker: New York, 1987; Chapter 5.
(35) Leermakers, F. A. M.; Scheutjens, J. M. H. M. *J. Colloid Interface Sci.* **1990**, *136*, 231.
(36) Jódar-Reyes, A. B.; Ortega-Vinuesa, J. L.; Martín-Rodríguez, A.; Leermakers, F. A. M. *Langmuir* **2002**, *18*, 8706.
(37) Eriksson, J. C.; Ljunggren, S. *J. Chem. Soc., Faraday Trans. 2* **1985**, *81*, 1209.
(38) May, S.; Ben-Shaul, A. *J. Phys. Chem. B* **2001**, *105*, 630.
(39) Karaborni, S.; Esselink, K.; Hilbers, P. A. J.; Smit, B.; Karthäuser, J.; van Os, N. M.; Zana, R. *Science* **1994**, *266*, 254.
(40) Candau, S. J.; Oda, R. *Colloids Surf., A* **2001**, *183*−*185*, 5.
(41) Couillet, I.; Hughes, T.; Maitland, G.; Candau, F.; Candau, S. J.
(42) *Langmuir* **2004**, *20*, 9550.
(43) Israelachvili, J.; Mitchell, D. J.; Ninham, B. W. *J. Chem. Soc., Faraday Trans. 2* **1976**, *72*, 1525.
(44) Cates, M. E.; Candau, S. J. *J. Phys.*: *Condens. Matter* **1990**, *2*, 6869.
(45) Kwon, S. Y.; Kim, M. W. *Curr. Appl. Phys.* **2002**, *2*, 71.
(46) Oda, R.; Narayanan, J.; Hassan, P. A.; Manohar, C.; Salkar, R. A.; Kern, F.; Candau, S. J. *Langmuir* **1998**, *14*, 4364.
(47) Kern, F.; Zana, R.; Candau, S. J. *Langmuir* **1991**, *7*, 1344.
(48) Oelschlaeger, Cl.; Waton, G.; Candau, S. J. *Langmuir* **2003**, *19-(25)*, 10495.
(49) Kern, F.; Lequeux, F.; Zana, R.; Candau, S. J *Langmuir* **1994**, *10*, 1714.
(50) Mazer, N. A.; Olofsson, G. *J. Phys. Chem.* **1982**, *86*, 4584.
(51) Porte, G. *J. Phys. Chem.* **1983**, *87*, 3541.
(52) Eriksson, J. C.; Ljunggren, S. *Langmuir* **1990**, *6*, 895.
(53) Han, L.; Chen, H.; Luo, P. *Surf. Sci.* **2004**, *564*, 141.
(54) Hurter, P. N.; Scheutjens, J. M. H. M.; Hatton, T. A. *Macromolecules* **1993**, *26*, 5592.
(55) Scheutjens, J. M. H. M.; Fleer, G. J. *J. Phys. Chem.*, **1979**, *83*, 1619.
(56) Scheutjens, J. M. H. M.; Fleer G. J. *J. Phys. Chem.* **1980**, *84*, 178.
(57) Evers, O. A.; Scheutjens, J. M. H. M.; Fleer, G. J *Macromolecules* **1990**, *23*, 5221.
(58) Schlangen, L. J. M.; Leermakers, F. A. M.; Koopal, L. K. *J. Chem. Soc., Faraday Trans.* **1996** *92*, 579.
(59) Jódar-Reyes, A. B.; Ortega-Vinuesa, J. L.; Martín-Rodríguez, A.; Leermakers, F. A. M. *Langmuir* **2003**, *19*, 878.
(60) Lauw, Y.; Leermakers, F. A. M.; Cohen Stuart, M. A. *J. Phys. Chem. B* **2003**, *107*, 10912.
(61) Goloub, T. P.; Koopal, L. K. *Langmuir* **1997**, *13*, 673.
(62) Corrin, M. L. *J. Colloid Sci.* **1948**, *3*, 333.
(63) Phillips, J. N. *Trans. Faraday Soc.* **1955**, *51*, 561.
(64) Mukerjee, P.; Mysels, K. J.; Dulin, C. I. *J. Phys. Chem.* **1958**, *62*, 1390.
(65) Israelachvili J. N. In *Intermolecular and Surface Forces*; Academic Press: London, 1991; Chapter 16.
(66) Romero-Cano, M. S.; Martın-Rodrıguez, A.; Chauveteau, G.; de las Nieves, F. J. *J. Colloid Interface Sci.* **1998**, *198*, 266.
(67) Molina-Bolıvar, J. A.; Aguiar, J.; Carnero Ruiz, C. *Mol. Phys.* **2001**, *99(20)*, 1729.
(68) Ruiz, C. C.; Molina-Bolıvar, J. A.; Aguiar, J.; MacIsaac, G.; Moroze, S.; Palepu, R. *Langmuir* **2001**, *17*, 6831.
(69) Kik, R. A.; Leermakers, F. A. M.; Kleijn, J. M. *Phys. Chem. Chem. Phys.* **2005**, *7*, 1996.
(70) Leermakers, F.; Eriksson, J. C.; Lyklema, H. In *Fundamentals of Interface and Colloid Science. Vol V*: *Soft Colloids*; Lyklema, H., Ed.; Elsevier: Amsterdam, 2005; Chapter 4.
(71) Porte, G. In *Micelles, Membranes, Microemulsions, and Monolayers*; Gelbart, W. M.; Ben-Shaul, A.; Roux, D. Ed.; Springer-Verlag: New York, 1994; Chapter 2.